Vol 17 No 2, February 2008
1674-1056/2008/17(02)/0608-10

Chinese Physics B

© 2008 Chin. Phys. Soc.
and IOP Publishing Ltd

The transient scattering mechanism of dipole array with reflector*

Zhang Xue-Qin(张雪芹)[a)b)†], Wang Jun-Hong(王均宏)[a)b)], and Li Zeng-Rui(李增瑞)[a)b)]

[a)] *Key Laboratory of All Optical Network & Advanced Telecommunication Network, Ministry of Education, Beijing* 100044, *China*
[b)] *Institute of Lightwave Technology, Beijing Jiaotong University, Beijing* 100044, *China*

(Received 8 May 2007; revised manuscript received 28 August 2007)

The transient backscattering mechanisms of a dipole array with reflector have been investigated from different aspects: time-domain, frequency-domain, and combined time-frequency domain, using 4×8 dipole arrays with reflector as an example. The data of scattering from the arrays under the incidence of Gaussian pulses are obtained by finite differential time domain method. The influences of the array structural parameters, incident wave parameters, and incident angles on the waveforms, spectrum, and time-frequency representations of the backscattered fields of the arrays are analysed and conclusions are drawn. From these characteristics and conclusions, it is possible to deduce the array structure inversely from the backscattered field.

Keywords: dipole array, reflector, scattering, time domain
PACC: 4110H, 4110F

1. Introduction

A dipole array with reflector is a kind of practical antennas used in radar. The analysis of electromagnetic scattering from the dipole array with reflector has already been studied in the past. Chu *et al*[1] studied the scattering of planar dipole arrays with sizes of 6×l5, 9×12 and 6×20 over finite ground planes by method of moment (MOM) and geometric theory of diffraction methods. Tittensor and Newton[2] studied the mono-static and bi-static scattering of 8 elements linear array and 9×9, 20×20 planar arrays fed by the isolated and non-isolated power divider using MOM. Wang and Gan[3] studied the in-band scattering of dipole arrays with edge loaded ground plane for reducing the back-scattering cross section by suppressing singular currents in reflector edges. With the trend toward ultra-wide bandwidth technology，researchers are interested in exploring the scattering properties of antenna arrays subject to the incidence of ultra-wide band waves or short pulses. In this aspect, Carin and Felsen[4] have studied the transient scattering of flat strip arrays by using a hybrid ray-(Floquet mode)-MOM algorithm; Wang *et al*[5,6] had studied the scattering characteristics of N parallel two-dimensional targets located in a Gaussian plane beam. In addition, a number of post-processing techniques are available for studying the scattering phenomena of different structures. Among these techniques, the joint time-frequency processing techniques can give more information about the scattering structures. A lot of works concerning the analysis of the scattering data obtained by joint time-frequency techniques have already been published.[7−17]

In this work, finite differential time domain (FDTD) method and perfect matched layer (PML) technique are used to calculate the scattering field of a 4×8 dipole array with reflector illuminated by Gaussian pulses from different directions. The mono-static scattering far field data are then analysed in both time-domain and frequency-domain. Furthermore, contributions of the dipoles and reflector of the array to the far scattered field are analysed separately. Finally, techniques of joint time-frequency processing based on the standard short-time Fourier transform (STFT) are employed to gain further insight of the scattering phenomena in time- frequency distribution. From these results, we can find the relationships between the array structure and the backscattered field.

*Project supported by the Foundations of Beijing Jiaotong University and the Scientific Research Foundation for the Returned Overseas Chinese Scholars, State Education Ministry.
†E-mail: 04111002@bjtu.edu.cn

2. Antenna structure and method of verification

The array considered in this paper is composed of a rectangular metallic reflector and a 4×8 dipole array, as shown in Fig.1. We assume that the array is designed to work at a centre frequency of 1 GHz. The length and radius of the dipoles are $0.5\,\lambda_0$ and $0.005\,\lambda_0$ respectively; and the distances between centres of adjacent dipoles are $0.6\,\lambda_0$ in collinear and $0.5\,\lambda_0$ in parallel. While the distance between dipoles and reflector is $0.25\,\lambda_0$, the latter has dimensions of $4.5\times3.8\,\lambda_0^2$. The dipoles are all terminated in the centre with an impedance of $Z_{\rm in} = 50 + {\rm j}0\Omega$. The incident electric field is a Gaussian pulse expressed as $E(t) = E_0\exp[-g^2(t-t_{\max})^2]$, where $E_0 = 1\,{\rm V/m}$, g is the Gaussian parameter, whose polarization is in the theta direction. And its the corresponding waveform and spectrum are shown in Fig.2.

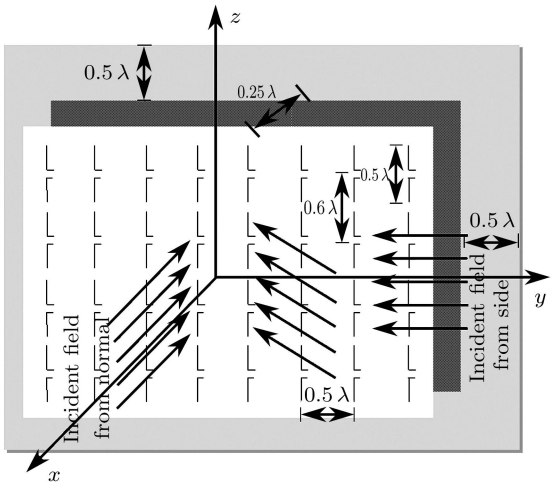


Fig.1. Antenna structure parameters and pulse incident direction.

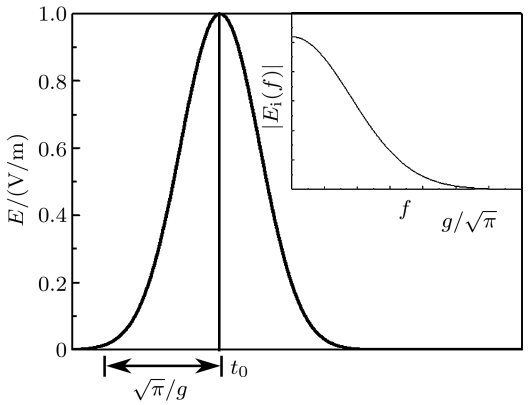


Fig.2. The waveform and spectrum of an incident pulse.

The scattered near field is obtained by FDTD, while the scattered far field is obtained by integrating the equivalent electrical and magnetic currents on an equivalent surface. To confirm the correctness of the code, the scattered pulse from a V-dipole with an included angle of 90° is calculated. The arm length and radius of the dipole are 1 m and 0.667 cm respectively, the same as those in Ref.[18]. A pulse is incident in the normal direction of the plane defined by two arms of the dipole, and the polarization of the electrical field is shown in Fig.3. In Ref.[18], the method based on time-domain integral equation is used, the Gaussian parameter g of the incident pulse being 1.5×10^9/s. The back scattered fields from our code and that in Ref.[18] are shown in Fig.3 for comparison. In the calculation, the grid size of FDTD is $\Delta x = \Delta y = \Delta z = 0.01$ cm, and the time interval is $\Delta t = \Delta x/(2c)$, where c is the velocity of light.

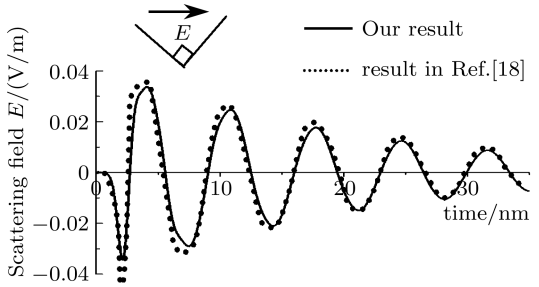


Fig.3. Backscattered field of a V-dipole under the incidence of Gaussian pulses with $g = 1.5\times10^9$/s.

3. Analysis of the data in time-domain

The situation of the antenna array and the incident field considered in this paper is shown in Fig.4, where dy and dz are the distances between centres of adjacent dipoles in y-direction and z-direction respectively, E_i and E_s are incident field and scattered field respectively. The path difference of radiation beams from two different dipoles to a far field point is $2N{\rm d}z\cos\theta + 2M{\rm d}y\sin\varphi\sin\theta$, and consequently the time delay is

$$\Delta t = (2N{\rm d}z\cos\theta + 2M{\rm d}y\sin\varphi\sin\theta)/c. \qquad (1)$$

In $\theta = 90°$ plane, when $\varphi = 0°$, Δt equals zero, when $\varphi = 90°$, Δt reaches its maximum.

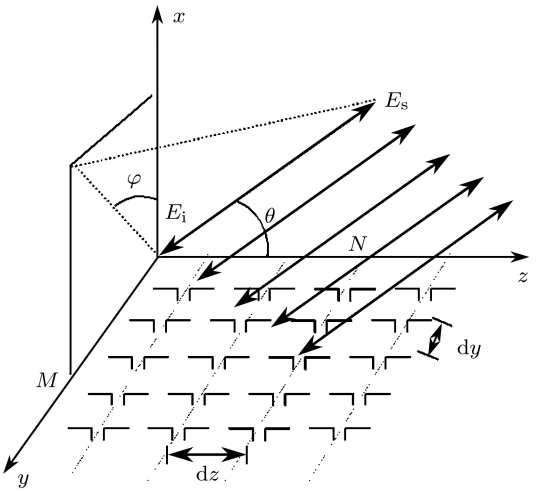


Fig.4. Sketch of the array and the field.

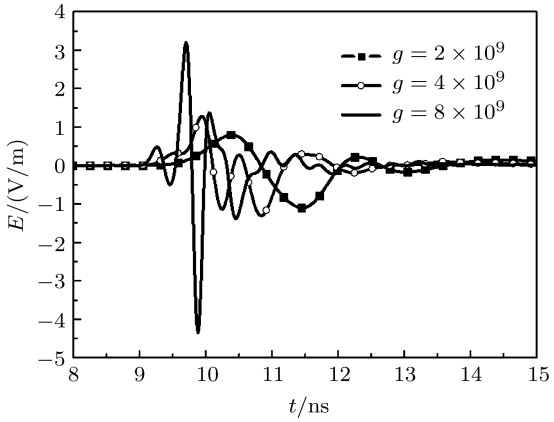


Fig.5. Time-domain waveform with impulse incident from $\theta = 90°$, $\varphi = 0°$.

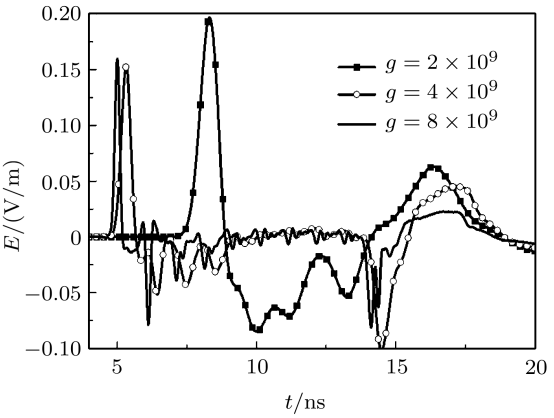


Fig.6. Time-domain waveform with impulse incident from $\theta = 90°$, $\varphi = 90°$.

Figures 5 and 6 show the backscattered time-domain waveforms of the 4×8 dipole array with reflector, in which the Gaussian pulses with $g = 2 \times 10^9$/s, 4×10^9/s and 8×10^9/s are incident from $\theta = 90°$, $\varphi = 0$ and $\theta = 90°$, $\varphi = 90°$ respectively. From Figs.5 and 6, we can see that the backscattered field is very strong when incident angle $\varphi = 0°$, this implies that the delay time between adjacent dipoles is equal to zero. While from Fig.6, we can see that the backscattered fields from dipoles cannot be added up in time when $\varphi = 90°$. There are two strong peaks (one positive and one negative) in the scattered waveform of $g = 8 \times 10^9$/s in Fig.6. In between the two strong peaks, there are eight small scattered pulses, and a time delay about $\Delta t = 1$ ns can be measured between these small pulses, which is consistent with the result of Eq.(1) for $d = 0.15$ m and $\theta = 90°$, $\varphi = 90°$. So these eight small scattered pulses exactly correspond to the eight rows of dipoles in y-direction. It is found from Fig.6 that only for the case of $g = 8 \times 10^9$/s, the scattered pulses from different dipole rows can be distinguished, while for other cases, it is not so clear. This is what expected because shorter pulse will give more information of the scatterer.

Whether the number of the rows of dipoles can be obtained from the scattered waveforms depends on the incident angle and the time span of the incident pulse. Figure 7 shows the scattered waveforms of the array with different incident angles and different widths of the pulse. The thresholds for distinguishing the dipole rows by using the scattered waves are summarized in Table 1. In the calculation, the threshold for the case of $g = 2 \times 10^9$/s cannot be determined, indicating that when $g \leq 2 \times 10^9$/s, the dipole rows cannot be distinguished by using the backscattered waveforms no matter what angle is, at which the wave is incident.

Table 1. Threshold values of the incident angle and Gaussian parameter g for determining the dipole number.

Gaussian parameter g/s	16×10^9	8×10^9	4×10^9	2×10^9
Incident angle φ/(°)	> 10	> 20	> 30	cannot be determined

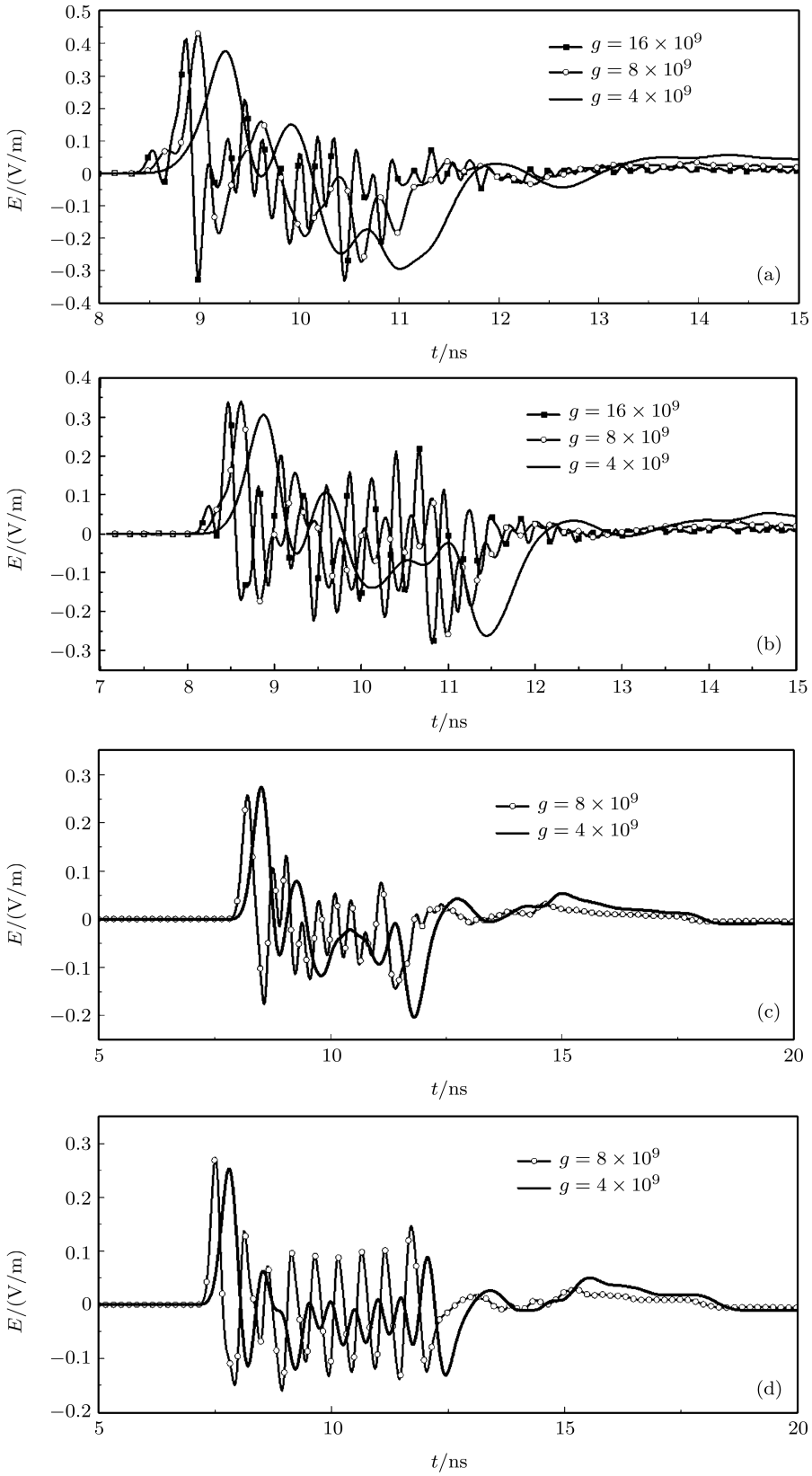


Fig.7. Time-domain backscattered waveform of the 4×8 dipole array with pulse incident from different angles. (a) $\theta = 90°$, $\varphi = 10°$; (b) $\theta = 90°$, $\varphi = 15°$; (c) $\theta = 90°$, $\varphi = 20°$; (d) $\theta = 90°$, $\varphi = 30°$.

From the limiting case shown in Fig.6 we find that the time intervals between two strong peaks (one positive and one negative) of the scattered waveforms for $g = 4 \times 10^9$/s and $g = 8 \times 10^9$/s cases are about 9 ns, which corresponds to a distance of 1.35 m according to Eq.(1). This distance is equal to the length of the reflector, so we can confirm that the two strong peaks are generated by the singular currents flowing in the reflector edges. This is similar to the frequency domain case where the singular currents generated in the reflector edges contribute a lot to overall radar cross section (RCS). In order to verify this, the length of reflector is increased to 1.65 m, the dipole array is kept unchanged, and the Gaussian pulse with $g = 8 \times 10^9$/s is incident from side direction; then a new backscattered waveform is obtained as shown in Fig.8. Compared with Fig.6, the eight scattered pulses due to the eight rows of dipoles in between two strong pulses are almost unchanged, but the time interval between the strong peaks is increased to $\Delta t = 11$ ns, which can be expected from Eq.(1). According to the above discussion, if the edge currents of the reflector are suppressed, then the two strong scattered peaks should be reduced. By loading the reflector edges with resistance, then the peak values of the currents in the edges can be suppressed as shown in Fig.9, in which the curves of peak value of the current along the y axis ($z = 0$) on the reflector with and without edge loading is given. When Gaussian pulse is incident from $\theta = 90°$, $\varphi = 90°$ and $g = 8 \times 10^9$/s. Fig.10 gives the corresponding backscattered waveforms. Comparing Fig.10 with Fig.6, we can observe that loading in reflector edges can significantly reduce the peak values of the back scattered pulse.

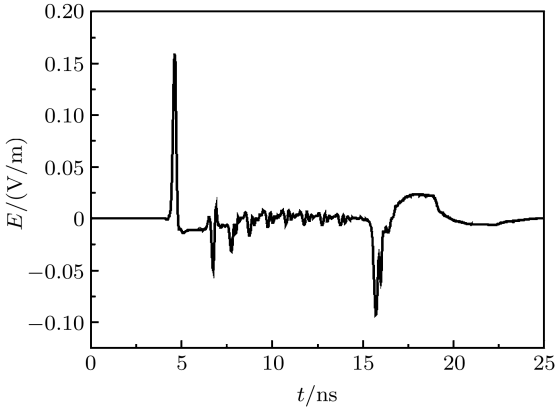


Fig.8. Backscattered waveform for the 4×8 dipole array with a larger length of reflector 1.65 m, $g = 8 \times 10^9$/s, $\theta = 90°$, $\varphi = 90°$.

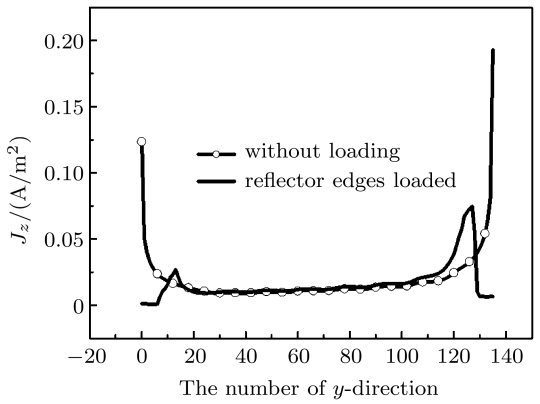


Fig.9. The curve of peak value of current along the y-direction ($z = 0$) of the reflector, for 4×8 dipole array at $g = 8 \times 10^9$/s, $\theta = 90°$, $\varphi = 90°$.

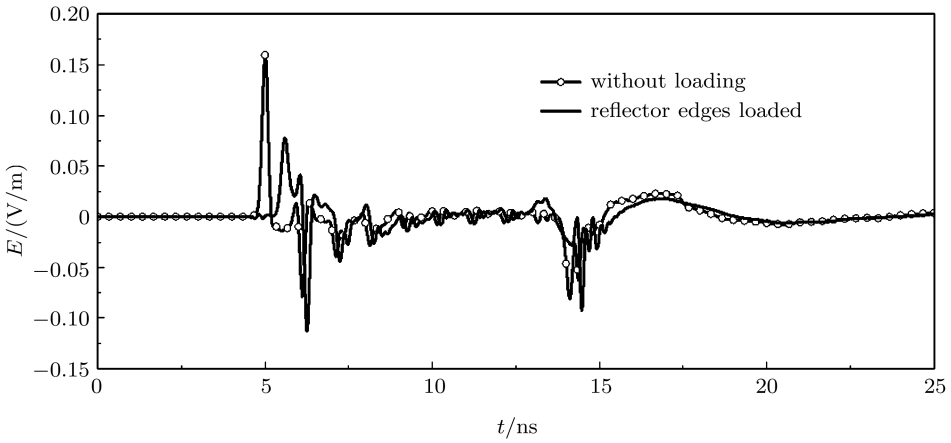


Fig.10. Backscattered waveform for 4×8 dipole arrays with and without reflector edge loading, parameters same as those in Fig.9.

In the above sections, the cases of pulse scattered in H-plane, i.e. the plane of $\theta = 90°$, are discussed. Figure 11 shows the backscattered waveform when Gaussian pulse with $g = 8 \times 10^9$/s is incident from $\theta = 0°$, $\varphi = 90°$ (E-plane). In this direction, because the current distribution in the z-axis of reflector has two peaks as shown in Fig.11(b), two strong peaks occur in the backscattered far field. Enlarge the section in between the two strong peaks, four small scattered pulses due to the four dipole rows can be found clearly.

Figures 12 and 13 show the backscattered waveform of a 8×16 dipole array with a $2.55 \times 1.71\,\mathrm{m}^2$ reflector, when Gaussian pulses with $g = 4 \times 10^9$/s and $g = 8 \times 10^9$/s are incident from $\theta = 90°$, $\varphi = 90°$ and $\theta = 0°$, $\varphi = 90°$ directions, respectively. From these two figures, the same conclusion as those for small arrays can be drawn.

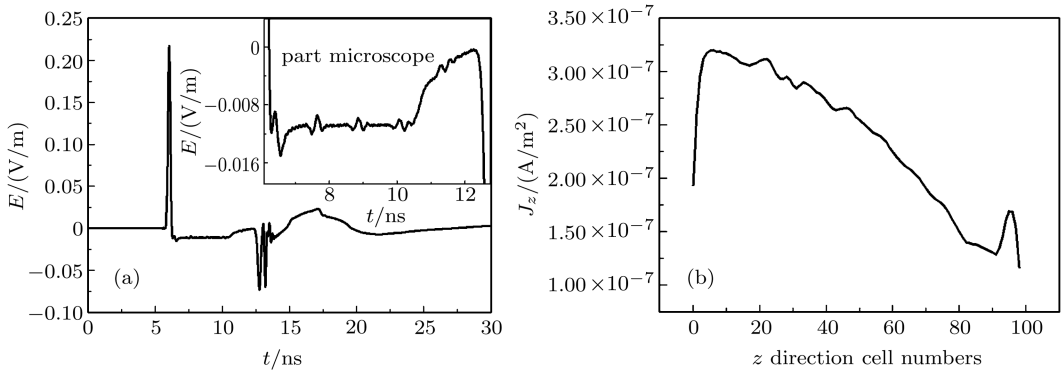


Fig.11. The backscattered waveform and current distribution on the reflector of the 4×8 dipole array. Gaussian pulse with $g = 8 \times 10^9$/s is incident from the direction of $\theta = 0°$, $\varphi = 90°$. (a) Backscattered waveform; (b) Peak value of current along z-direction ($y = 0$).

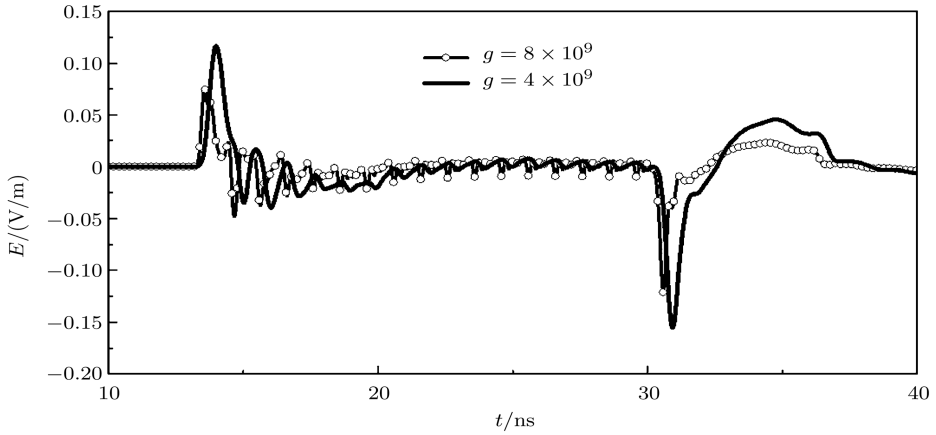


Fig.12. The backscattered waveform of a 8×16 dipole array with a 2.55×1.71 m^2 reflector, with $g = 4{\times}10^9$/s, $\theta = 90°$, $\varphi = 90°$.

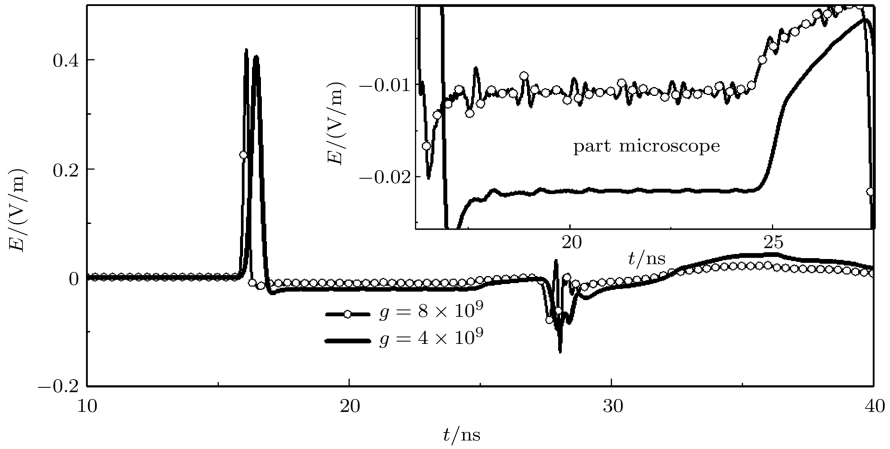


Fig.13. The backscattered waveform of a 8×16 dipole array with a 2.55×1.71 m^2 reflector, with $g = 4{\times}10^9$/s, $\theta = 0°$, $\varphi = 90°$.

4. Analysis of the data in frequency-domain

From Fig.4 we know that the phase differences ψ of the backscattered fields from the two dipoles in y- and z- directions are respectively

$$\psi_y = 2Mk\mathrm{d}y\sin\varphi\sin\theta,$$
$$\psi_z = 2Nk\mathrm{d}z\cos\theta, \tag{2}$$

where $k = 2\pi/\lambda$ is the propagation constant. As is known, the array factor of a plane array is

$$F(\psi) = \frac{\sin(M\psi_y/2)}{M\sin(\psi_y/2)} \cdot \frac{\sin(N\psi_z/2)}{N\sin(\psi_z/2)}. \tag{3}$$

Here we mainly consider the pulse scattered in H-plane, i.e. the plane of $\theta = 90°$. When $M\psi_y/2 = n\pi$, that is, $Mk\mathrm{d}y\sin\varphi = n\pi$, $n = 1, 2, 3, \cdots$ and $n \neq M, 2M, 3M, \cdots, F(\psi)$ equals zero, while $n = M, 2M, 3M, \cdots, F(\psi)$ reaches its maximum. In other words, when

$$f = \frac{c}{\lambda} = \frac{nc}{2M\mathrm{d}y\sin\varphi}, \quad n = 1, 2, 3, \cdots, \quad n \neq M, 2M, 3M, \cdots, \tag{4}$$

the backscattered field has its minimum, and when $n = M$, $2M$, $3M$, $\cdots$, the backscattered field has its maximum.

For a 4×8 dipole array with reflector, the spectra of the backscattered fields with $g = 4 \times 10^9$/s and $g = 8 \times 10^9$/s are shown in Figs.14 and 15, respectively, for normal incident and side incident Gaussian pulses. From Fig.14, we can see that the nulls appear

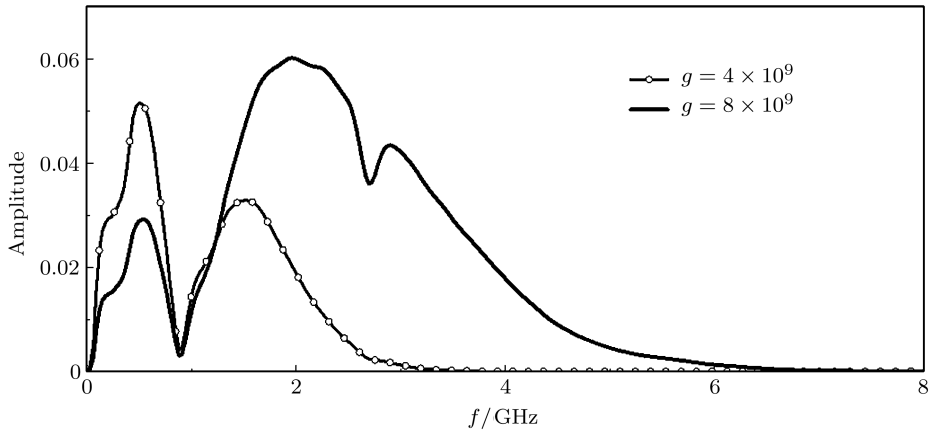


Fig.14. The spectrum of the backscattered field of a 4×8 dipole array when Gaussian pulse is incident from the normal direction.

near 1.0 GHz and 3.0 GHz. The reason for this is that when the pulse is incident from the normal direction, the backscattered fields from the dipoles and from the reflector cancel each other, and nulls will occur around frequencies of 1.0 GHz and 3.0 GHz. When the pulse is incident from side direction i.e. $\theta = 90°$ and $\varphi = 90°$, according to Eq.(4), the spectrum around 1.0 GHz should have a peak, and cannot be a null as shown in Fig.15. This is due to the effect of singular currents induced in the reflector edges, as pointed out

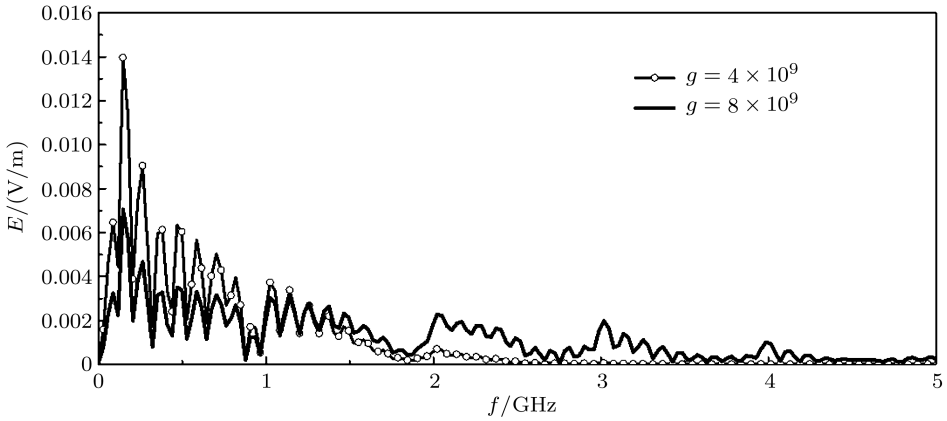


Fig.15. The spectrum of the backscattered field of a 4×8 dipole array when Gaussian pulse is incident from $\theta = 90°$, $\varphi = 90°$.

in section 3. Seven nulls will appear at frequencies around 0.125, 0.25, 0.375, 0.50, 0.625 , 0.75 and 0.875 GHz in between 0 and 1.0 GHz, and other seven nulls will appear in between 1.0 and 2.0 GHz, 2.0 and 3.0 GHz, and so on. Figure 16 shows the spectrum of the backscattered field of the dipole array with reflector edges loaded with resistance when Gaussian pulse with $g = 8 \times 10^9$/s is incident from $\theta = 90°$, $\varphi = 90°$. From Fig.16, we can see that the null at 1 GHz now changes to peak because the suppression of the singular reflector edge current, and the scattered energy in the low-frequency band becomes smaller. This implies that the reflector edges contribute a lot to the scattering in low-frequency band.

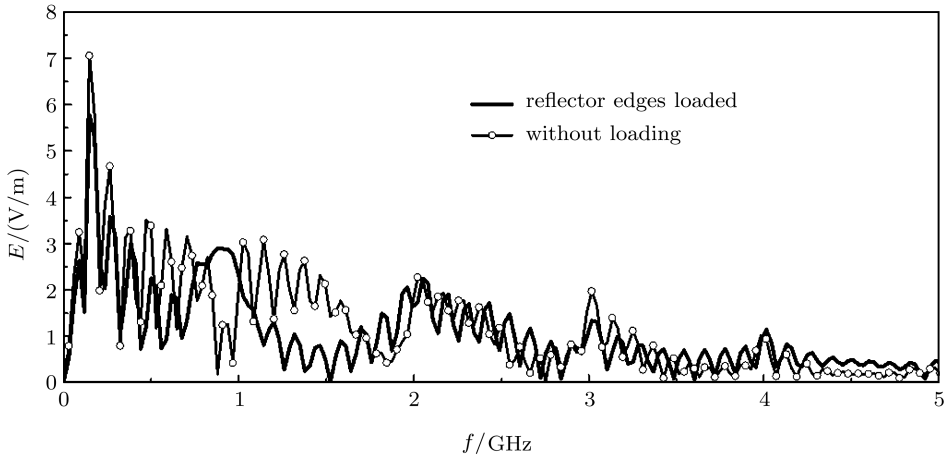


Fig.16. The spectrum of the backscattered field of a 4×8 dipole array when Gaussian pulse with $g = 8\times10^9$/s is incident from $\theta = 90°$, $\varphi = 90°$.

5. Time-frequency characteristics of the scattered field

Transient scattering of a dipole array with reflector contains both in-band and out-band scattering information. Time-frequency processing technique using short-time Fourier transform (STFT) is a powerful tool to interpret the scattering phenomena. The STFT of a signal, or its spectrogram, takes the Fourier transform of a windowed part of the signal either in time domain or in frequency domain. In time domain, the Gaussian-windowed STFT of a function $g(t)$ is expressed as[13]

$$G(\omega,\tau;\sigma) = \frac{1}{\sqrt{2\pi}\sigma}\int_{-\infty}^{\infty} g(t)\exp(j\omega t) \times \exp\left[-(t-\tau)^2/2\sigma^2\right]\mathrm{d}t, \quad (5)$$

where τ is the centre position of the sliding Gaussian window with a standard deviation σ, which is a measure of the width of its Fourier transform. When σ is decreased, the width of the window will also be decreased. Due to the uncertainty relationship between the window functions in time domain and in frequency domain, a higher resolution can be achieved in one domain by using a wide window in the other domain. Hence, window width should be selected properly to give the spectrogram with a sufficient good resolution. In this paper, σ is selected to be 0.4. Point Gaussian window equal to 1/4 pulse width has been chosen, as shown in time-frequency representation.

Figure 17 shows the time-frequency representation of the backscattered field of the dipole array with reflector when the Gaussian pulse with different widths is incident from the normal direction $\theta = 90°$, $\varphi = 0°$. The minimum points in frequency domain appear at frequencies of 1, 3, 5 and so on, and the group delay time cannot be found in Fig.16; this is consistent with the time-domain and frequency- domain analyses. Figure 18 shows the time-frequency representation of the backscattered field of the array with reflector when the Gaussian pulse with different widths is incident from $\theta = 90°$, $\varphi = 90°$. From Fig.18 we can see that the signal in low-frequency band is stronger and the time delay is longer than those in high-frequency band. Figure 19 presents the case for the array without reflector. This figure shows that the low-frequency signal with a longer time delay dis-

appears, and the centre frequency for the maximum backscattered field occurs at 1 GHz and its multiple. Since the sampling rate is not so high, only the maximum point can be distinguished. The time-frequency representation indicates again that the reflector is a main contributor to the total scattering.

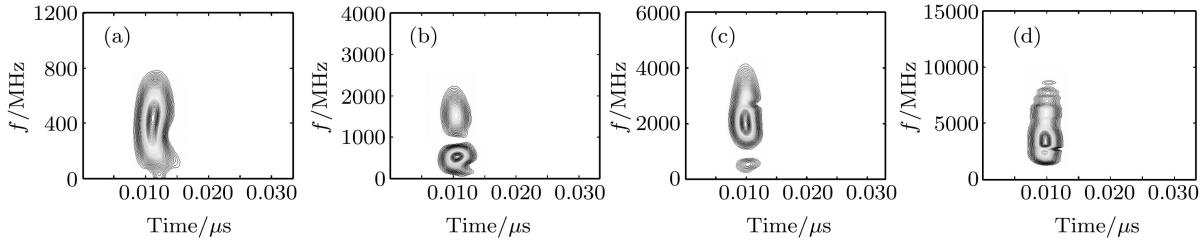


Fig.17. Time-frequency representation of the backscattered field of the 4×8 array when the Gaussian pulse is incident from $\theta = 90°$, $\varphi = 0°$. (a) $g = 2 \times 10^9$/s; (b) $g = 4 \times 10^9$/s; (c) $g = 8 \times 10^9$/s; (d) $g = 16 \times 10^9$/s.

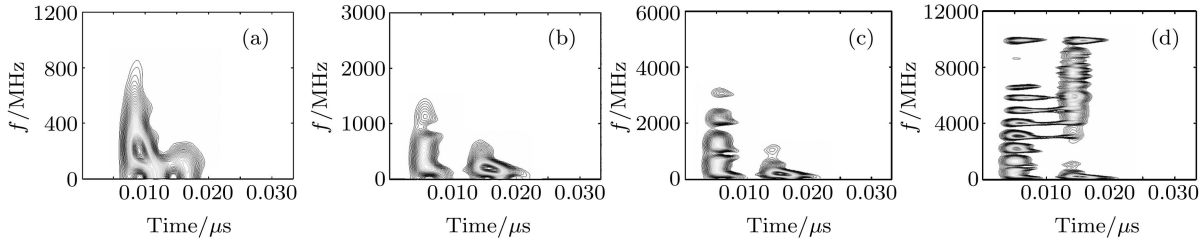


Fig.18. Time-frequency representation of the backscattered field of the 4×8 array when the Gaussian pulse is incident from $\theta = 90°$, $\varphi = 90°$.(a) $g = 2 \times 10^9$/s; (b) $g = 4 \times 10^9$/s; (c) $g = 8 \times 10^9$/s; (d) $g = 16 \times 10^9$/s.

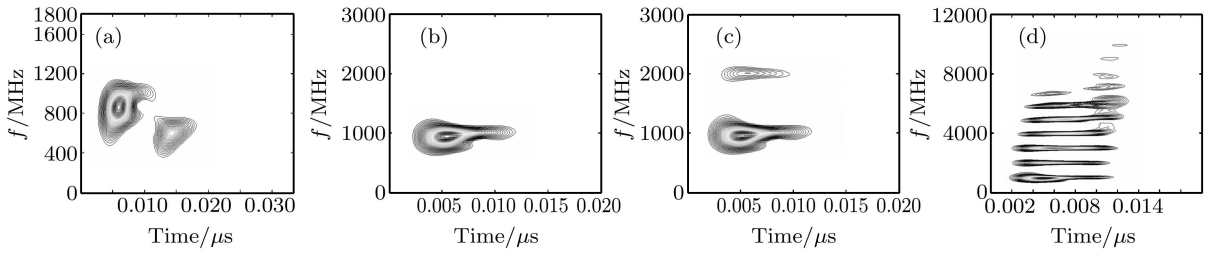


Fig.19. Time-frequency representation of the backscattered field of the 4×8 array without reflector when the Gaussian pulse is incident from $\theta = 90°$, $\varphi = 90°$ (a) $g = 2 \times 10^9$/s; (b) $g = 4 \times 10^9$/s; (c) $g = 8 \times 10^9$/s; (d) $g = 16 \times 10^9$/s.

6. Conclusions

Incident pulses have the characters of short time span in time domain and wide frequency band in spectrum domain. Therefore, the mono-static transient scattering field of a dipole array with reflector contains a great deal of information. From the above analyses, we find that for a reflector-backed dipole array, the scattered pulses from the reflector edges are stronger than those from the dipoles. It seems that the reflector contributes a lot to the backscattered far field, especially in low-frequency band. When the reflector edges are loaded, the scattering from the reflector is significantly reduced. In addition, when the pulse with very short time width is incident from a certain range of angles, the array structure can be inversely deduced from the time-domain waveforms, frequency spectra, and the time-frequency representations.

References

[1] Chu R S, Jenn D C and Wong N S 1987 *IEEE Antenna and Propagation Symposium* **11** 722

[2] Tittensor P J and Newton M L 1989 *Newton Sixth International Conference on Antennas and Propagation*(ICAP 89) **1** 258

[3] Wang J H and Gan Y B 2003 *IEEE Antennas and Propagation Society International Symposium* **4** 468

[4] Carin L and Felsen L B 1993 *IEEE Transactions on Antennas and Propagation* **41** 412

[5] Wang Y H, Guo L X and Wu Z S 2007 *Acta Phys. Sin.* **56** 186 (in Chinese)

[6] Wang Y H, Guo L X and Wu Z S 2006 *Chin. Phys.* **15** 1755

[7] Strifors H C, Gaunaurd G C, Abrahamsson S and Brusmark B 1993 *IEEE National* 1993 70

[8] Luiz C T and Hao L 1995 *IEEE Trans. Antennas Propagat.* **43** 1253

[9] Caner O and Hao L 1997 *IEEE Trans. Antennas Propagat.* **45** 1259

[10] Moghaddar A and Walton E K 1993 *IEEE Trans. Antennas Propagat.* **41** 677

[11] Kralj D R, McClure M, Carin L and Felsen L B 1994 *Antennas and Propagation Society International Symposium* **11** 2685

[12] Kim H and Ling H 1993 *IEEE Trans. Antennas Propagat.* **41** 200

[13] Carin L and Felsen L B 1994 *IEEE Antennas Propagat.* **36** 29

[14] Carin L, Felsen L B and Kralj David R 1997 *IEEE Antennas Propagat.* **45** 592

[15] Cohen L 1989 *Proc. IEEE* **77** 941

[16] Li N, Zhang T, Lü X L and Zhang S H 2006 CIE'06. International Conference 1.

[17] Bai B D, Xie D X, Yao Y Y and Zeng L S 2001 *Proc. Fifth International Conference on Electrical Machines and Systems* **2** 1184

[18] Mittra R 1973 *Computer Techniques for Electromagnetics* (Oxford: Pergamon) p259